Journal of Oceanography and Marine Research

Umesh and Swain, J Oceanogr Mar Res 2018, 6:1
DOI: 10.4172/2572-3103.1000173

Research Article Open Access

Prediction of Uncertainty Using the Third Generation Wave Model WAVEWATCH III Driven By ERA-40 and Blended Winds in the North Indian Ocean

Swain J[1] and Umesh PA[1,2]*

[1]Naval Physical and Oceanographic Laboratory, Thrikkakara P.O., Kochi - 21, India
[2]Department of Ocean Engineering & Naval Architecture, Indian Institute of Technology Kharagpur, Kharagpur - 721 302, West Bengal, India

Abstract

Simulation of waves in North Indian Ocean using ERA-40 and QuikSCAT/NCEP blended winds over 1° × 1° grid resolutions has been realised globally as well regionally using the third-generation wave model WAVEWATCH III (WWIII). Moreover, the model performance was evaluated by quantifying the uncertainty`s. So, WWIII simulations have been carried out for the North Indian Ocean from 50°E to 100°E and 0°N to 30°N with the past analysed winds (hindcasting) and the boundary conditions from the global run. The model outputs such as significant wave height (Hs) and mean wave period (Tc) are compared with the buoy measurements. To assess the performance, various statistical errors have been estimated by validating the model results against moored buoy data in the Arabian Sea and Bay of Bengal. The validation of WWIII with buoy measurements gave promising results for the North Indian Ocean with Model Performance Index ranging from 0.86 to 0.99, irrespective of the input winds. Also, Percentage Error ranges from 3.1 to 18.8% for the selected periods (January, July and October) except April. Further, the model was examined with different wind forcing's and the study revealed better performances with blended winds, which could accurately predict Hs and Tc at buoy locations. This study concludes that, WWIII model predicts the sea-state evolution with acceptable uncertainty, which is reliable for the Indian Seas (North Indian Ocean) using the analysed wind fields. Further, better accuracy is achieved using blended wind products.

Keywords: WAVEWATCH; ERA-40; WWIII; Model uncertainty; Wave hindcasts; Validation; Blended Winds

Introduction

In civilian and defence sectors, the wind-induced surface gravity waves have wide-range applications. In the reports of Richard et al. [1] Umesh et al. [2] Swain et al. [3] we can conclude that the design of coastal and offshore structures, optimum tracking of surface and subsurface vehicles management, search and rescue operations during rough weather depends on the available wave information. In addition, it is also required for the protection of coastal zone, assessment, and exploitation of wave power potential, towing of underwater bodies, detection and discrimination of underwater objects. The sea-state also has a dominant role in the air-sea interaction processes of the coupled ocean-atmosphere system while predicting the future weather. Keeping these in mind, it is necessary that one should aim at predicting the sea-state and its uncertainty in prediction orin the evolution of sea surface waves using the available state-of-the-art wave models [4-7] for the region of interest. With the increasing demand for modernization, there is equally an increasing demand to forecast ocean waves [8] in open sea and coastal areas to aid marine applications. Literature [9-11] indicates that high number of users including the scientific community depend on nowcasts and ocean state forecasts for marine related operations In this regard, it has become feasible to undertake the routine wave nowcast and forecast for the Indian Ocean utilising the analysed and forecast winds respectively. Therefore, before attempting the same, it is essential to validate the model to be used for routine wave prediction [12-14]. This can be attempted in two ways, either in operational mode or through hindcasting. The model used in this study is the third-generation wave model WWIII [15] which is implemented at Naval Physical and Oceanographic Laboratory (NPOL) for the North Indian Ocean for research purpose and for operational applications.

The results of WWIII hindcast presented in this study was one of the collaborative research programme between NPOL (DRDO) and Space Application Centre (ISRO) for wave hindcasting in the Indian Ocean utilising the ERA-40 and QuikSCAT/NCEP blended winds. For significant improvement on the model's performance, it is validated utilizing data from few representative locations in the North Indian Ocean. The model has been validated with field measurements during different seasons of the year representing different wind and wave characteristics. Also, the sensitivity of the model with different wind forcing's examined. Uncertainty in the present context is the evaluation of wave model and its performance predictions using the reliable input fields.

The Wave Model

The WWIII wave model (version 3.14) implemented here for the global as well as regional domain is capable of segregating swells from the total energy spectrum of the sea-state, and hence can provide a wide array of ocean wave parameters as output. WWIII is basically an extension of WAM wave model, which is developed at NOAA/NCEP [15,16]. It has been successfully applied in global and regional scale studies in many areas including the North Atlantic, and it has proven to be an effective tool to study wave spectral evolution, air-

***Corresponding author:** Umesh PA, Department of Ocean Engineering & Naval Architecture, Indian Institute of Technology Kharagpur, Kharagpur-721302, West Bengal, India, Tel: +91-3222-255221 and Fax: +91-3222-255303; E-mail: umeshpa.nair@gmail.com, umesh@naval.iitkgp.ernet.in

Received August 31, 2017; **Accepted** January 29, 2018; **Published** February 12, 2018

Citation: Swain J, Umesh PA (2018) Prediction of Uncertainty Using the Third Generation Wave Model WAVEWATCH III Driven By ERA-40 and Blended Winds in the North Indian Ocean. J Oceanogr Mar Res 6: 173. doi: 10.4172/2572-3103.1000173

sea interactions and nonlinear wave-wave interactions. WWIII is a discrete spectra and phase averaged model [17]. For the regional and global applications, the directional wave spectrum is resolved at ever grid point across wavenumber-direction bands. By numerically solving the spectral wave action balance equation (1), the evolution of the wave field is achieved:

$$\frac{\partial N}{\partial t}+\frac{1}{\cos\phi}\frac{\partial}{\partial\phi}\dot{\phi}N\cos\theta+\frac{\partial}{\partial\lambda}\dot{\lambda}N+\frac{\partial}{\partial k}\dot{k}N+\frac{\partial}{\partial\theta}\dot{\theta}_g N=\frac{S}{\sigma} \quad (1)$$

$$\dot{\phi}=\frac{c_g\cos\theta+U_\phi}{R}$$

$$\dot{\lambda}=\frac{c_g\sin\theta+U_\lambda}{R\cos\phi} \quad (2)$$

$$\dot{\theta}_g=\dot{\theta}-\frac{c_g\tan\phi\cos\theta}{R}$$

Where, λ is longitude, φ is latitude, θ is wave propagation direction, *k* is wave number, *t* is time, σ is the intrinsic angular frequency. R is the radius of the earth, and U_φ and U_λ are current components in φ and λ directions. The left side of equation (1) represents the local rate of change of wave action density, propagation in physical space, action density shifting in frequency and direction due to the spatial and temporal variations of depth and current.

In deep waters, the net source term S is generally considered to consist of three parts, a wind-wave interaction term S_{in}, a nonlinear wave-wave interaction term S_{nl} and a dissipation (whitecapping) term S_{ds}. The input term S_{in} is dominated by the exponential growth term, and the source term generally describes this dominant process only. For model initialization and to provide more realistic initial wave growth, and linear input term S_{ln} is also considered in WWIII. In shallow waters, additional processes are mostly notably wave-bottom interactions, S_{bot} [18]. In near-shore waters, depth-induced breaking (S_{db}) and triad wave-wave interactions (S_{tr}) are considered. WWIII also caters for the source terms for scattering of waves by topographic features (S_{sc}) and a general-purpose slot for additional, user defined source terms (S_{xx}).

The general source terms used in WWIII is defined as:

$$S = S_{ln} + S_{in} + S_{nl} + S_{ds} + S_{bot} + S_{db} + S_{tr} + S_{sc} + S_{xx} \quad (3)$$

Two combinations of the source terms S_{in} and S_{ds} (input and dissipation due to white capping) are available in WWIII. The default set up of WWIII corresponds to the wave-boundary layer formulation for S_{in} and S_{ds} by Tolman and Chalikov [16]. The alternate combination corresponds to WAM Cycle-3 physics (WAMC3 physics), in which S_{in} and S_{ds} are based on WAMDI, Snyder et al. and Komen et al. In both cases, the source terms are integrated in time using a dynamically adjusted time stepping algorithm, which concentrates computational efforts on conditions with rapid spectral changes [6]. Quadruplet nonlinear interactions S_{nl} are simulated using the Discrete Interaction Approximation (DIA) [19,20] and bottom dissipation S_{bf}, by the JONSWAP parameterization of Hasselmann et al. [21]. A simple upwind scheme is used in WWIII for propagation. First or third order accurate numerical schemes are available to describe wave propagation which are linear, while relevant nonlinear effects such as resonant interactions are included in the source terms. Wave spectrum is discretized using a constant directional increment (covering the entire circle), and a spatially varying wavenumber grid.

Data and Methodology

Wind data

Acccurate wind fields are needed for better wave prediction. Selecting the appropriate wind data with sufficient spatio-temporal resolution over a global domain is a major task, which greatly determines the reliability and accuracy of wave model results. The two sets of wind products used in this study are the ERA-40 winds and the QuikSCAT/NCEP blended windfields. ECMWF 40 Year Reanalysis (ERA-40) is a reanalysis of meteorological observations from September 1957 to August 2002 (45 years), released by ECMWF [22]. One of the products of ERA-40 consists of 6-hourly global fields of wind speed at 10 metres height (U_{10}) with a 1.5° × 1.5° grid resolution. In this study, the wind speed, and the stresses for the year 2000 was extracted from ERA-40 and the same was used to estimate wind direction; and the winds were further interpolated to 1° × 1° grid resolution. The QuikSCAT/NCEP blended wind products were derived through a spatial blending of the high-resolution scatterometer (QuikSCAT) wind observations with the NCEP/NCAR reanalysis winds [23,24]. The NCEP/NCAR analysis fields are the products of the NCEP Climate Data Assimilation System (CDAS), which was an operational system developed for the NCEP-NCAR reanalysis [25]. These data files (6-hourly, 0.5° × 0.5°) available from the NCAR Data Support Section (DSS): DS744.4 - QSCAT/NCEP Blended Ocean Winds; is used and interpolated to 1° × 1° (model grid resolution) for wave hindcasting.

Wave data in the Arabian Sea and Bay of Bengal

The National Data Buoy Programme (NDBP) was implemented in 1997 at the National Institute of Ocean Technology (NIOT), Chennai, India under the Ministry of Earth Sciences (MoES), India to bring out real-time meteorological and oceanographic observations [26]. Many moored buoys were deployed in the Arabian Sea and Bay of Bengal [27,28]. The *in situ* observations from 9 locations (Figure 1), representing both the Arabian Sea and the Bay of Bengal, have been used in this study, for validating the WWIII results. These moored buoys have a motion reference unit for wave measurements. The data was measured at the rate of 1 Hz for 17 min at every 3 h duration. The details of the buoy locations, depth and the period of data used is as shown in Table 1. These buoys are operable from 20 m water depths to full ocean depth, excepting few buoys, which are also functional slightly at lower depths. The sensor used in the measurement of wave parameters is an inertial altitude heading reference system

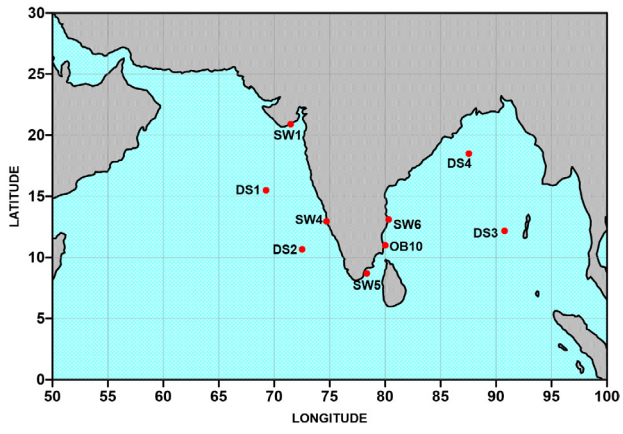

Figure 1: Locations of NIOT buoy measurements in the Indian Seas utilized for WWIII validation.

Sl. No.	BUOY	LOCATION		DEPTH (m)	PERIOD OF DATA USED
		Lat. (^{0}N)	Long. (^{0}E)		
1.	**DS1** *(off Goa)*	15.51	69.25	3800	01-31 January 2000, 01-30 April 2000, 01-31 July 2000, 01-31 October 2000
2.	**DS2** *(off Lakshadweep)*	10.67	72.51	1800	01-31 January 2000, 24-30 April 2000 01-31 July 2000, 01-31 October 2000
3.	**SW1** *(off Pipavav port)*	20.89	71.49	24	01-31 January 2000, 01-23 April 2000 01-31 July 2000, 01-31 October 2000
4.	**SW4** *(off Mangalore port)*	12.93	74.72	24	01-31 January 2000, 03-30 April 2000 01-31 July 2000, 01-29 October 2000
5.	**DS3** *(off Andaman & Nicobar)*	12.15	90.75	3100	01-31 July 2000, 01-31 October 2000
6.	**DS4** *(off Paradip)*	18.48	87.55	2300	01-31 October 2000
7.	**SW5** *(off Tuticorin port)*	8.69	78.34	24	01-31 January 2000, 01-30 April 2000, 01-31 July 2000, 01-31 October 2000
8.	**SW6** *(off Chennai port)*	13.10	80.33	16	01-30 April 2000, 01-31 July 2000 01-31 October 2000
9.	**OB10** *(off Chidambaram)*	11.00	80.00	36	01-31 January 2009

Table 1: Details of moored buoys utilized for validation of WWIII.

with dynamic linear motion measurement capability. The waves are measured in the buoy by a motion reference unit, which measures absolute roll, pitch, yaw and relative heave. These data are recorded at a rate of 1 Hz for 17 min every three hours. It measures the full spectrum of the waves for 17 min. The Significant wave height is estimated as four times the square root of the area under the non-directional wave spectrum. It has an accuracy ± 10 cm for wave height up to 20 m and ± 5° for wave direction. In this study, wave data measured at deepwater locations such as DS1 (off Goa) during January, April, July and October 2000, DS2 (off Lakshadweep) during January, April, July and October 2000, DS3 (off Andaman & Nicobar) during July and October 2000, DS4 during October 2000, OB10 (off Chidambaram) during January 2009 and SW1 at shallow water locations off Pipavav port during January, April, July and October 2000, SW4 (off Mangalore port) during January, April, July and October 2000, SW5 (off Tuticorin port) during January, April, July and October 2000 and SW6 (off Chennai port) during April, July and October 2000 are utilized for the validation of wave model (WWIII) hindcasts.

Model Set up and Methods

The WWIII version 3.14 from NOAA [15] was implemented for simulating waves over the gridded bathymetry for the whole globe using analysed winds. The global grid system covers the geographical extend 0^0 to 360^0E and 77^0S to 77^0N with a resolution 1°x1°. The bathymetric map has been constructed from ETOPO2 data. The model uses 25 frequencies ranging from 0.0412 Hz to 0.4056 Hz, with a logarithmic distribution with increment factor 1.1 and 24 directions (constant increment). The wave model was executed for the whole global grid, whereas it was set to generate boundary outputs for the regional model domain of North Indian Ocean (50^0E to 100^0E; 0^0N to 30^0N). Source integration and propagation time steps were set to 10 minutes and 20 minutes; and 5 minutes and 15 minutes respectively for the global and regional model executions. The time splitting scheme in WWIII with four different time steps solves the physical processes to save computational time. The global time step used in WWIII is the maximum time step for source term integration, and used by the input winds to propagate the solution to neighbouring grids. The propagation along spatial dimension is solved using a third-order accurate scheme, wherein the time step can be smaller or equal to the global time step. The intra-spectral propagation uses the third order accurate scheme. The numerical integration of source terms uses a modified version of semi-implicit scheme. To achieve computational efficiency, the maximum propagation step is set to 20 minutes for longest wave (CFL time step X-Y) components in the spectrum and refraction step (CFL time step k-theta) is 30 minutes.

The wave model was driven with ERA-40 and QuikSCAT/NCEP Blended winds; air-sea temperature difference (ERA-interim daily fields from ECMWF were used to extract the air-sea temperature difference data) and OSCAR surface currents [29] with similar resolutions of $1^{\circ} \times 1^{\circ}$ longitude-latitude grids. The WWIII model outputs for various wave parameters were stored every 6-hourly. Two case studies have been carried out for analysed winds (Case-I: January, April, July and October 2000) using ERA-40 winds and another (Case-II: July 2008 and January 2009) using QuikSCAT/NCEP Blended winds. The months of January, April, July and October 2000 were chosen with the consideration that January and July are the peaks of northeast and southwest monsoon respectively; and April and October are the pre-and post-monsoon months/periods respectively. The error analysis and validations of hindcast wave parameters have been carried out using the buoy data of NIOT (DS1, DS2, DS3, DS4, SW1, SW4, SW5, SW6, OB10). For an assessment of uncertainty in prediction, the most important statistical measures such as Coefficient of Correlation (R), Scatter Index (SI), Bias (B, Mean Deviation), Root Mean Square Error (RMSE), Percentage Error (PE) and Model Performance Index (MPI) between measurements and model outputs have been computed and examined to evaluate the model performances as indicated below where 'm' represents model values and 'obs' represents observed/measured values [30-34].

$$\text{Bias} = \frac{1}{n}\sum(\text{m} - \text{obs}) \tag{4}$$

$$RMSE = \sqrt{\frac{1}{n}\sum(m - obs)^2} \tag{5}$$

$$SI = \frac{RMSE}{(\overline{obs})} \tag{6}$$

$$\text{R} = \frac{\sum(\text{m} - \overline{\text{m}})\,(\text{obs} - \overline{\text{obs}})}{\sqrt{\sum(\text{m} - \overline{\text{m}})^2\,(\text{obs} - \overline{\text{obs}})^2}} \tag{7}$$

$$\text{MPI} = 1 - \frac{\text{rms}_{\text{error}}}{\text{rms}_{\text{changes}}} \tag{8}$$

Results and Discussion

The wind and wave conditions in the Arabian Sea and Bay of Bengal (Indian Seas or North Indian Ocean) are generally high during

the south-west monsoon [35,36] and low during north-east monsoon, which is considered to be the rough weather and fair-weather seasons from wave climate point of view. Six-hourly analysed fields were utilized as inputs to force the WWIII model for wave hindcasting during January, April, July and October 2010 (Case-I); and July 2008 and January 2009 (Case-II). The analysis based on both these cases are described below. The case studies on validation of WWIII results using measurements presented in this study belong to the rough weather and fair weather periods.

Wave Hindcasts - Case I: January, April, July and October 2000

In this case study (Case-I), ERA-40 analysed winds have been used as input to force the WWIII model for the four selected months such as January, April, July and October 2000. The spatial distribution of sample input wind fields for the North Indian Ocean for the day (25th, 1200 h of each month) is shown in Figure 2 followed by a brief analysis of prevailing wind and the hindcast waves. Figure 2a-d shows the wind speed and direction at 1200 h of 25 January, 25 April, 25 July and 25 October 2000, respectively. Reasonably strong winds ranging 4 to 9 m/s with direction around northeast prevailed on 25 January, being the fair weather season. Higher winds around 9 m/s were seen in south central Bay. During April, the winds are generally low and variable. However, relatively higher winds were seen (around 7-9 m/s) in southwestern Bay and northern extreme of Arabian Sea on 25 April 2000, 1200 h, which is likely to be the pre-monsoon activity. It may be specifically noted from the Figure 2c that the normal southwest monsoon winds were active all over the North Indian Ocean with speed ranging from 6-10 m/s, and the noticeable stronger jet being off the Somalia coast. A weak low pressure system was noticed in the central Bay with higher westerly winds (6-8 m/s) around southeast Arabian Sea and southern parts of Bay of Bengal (Figure 2d).

The spatial distributions (contour plots) of significant wave height (Hs), mean wave period (Tc), swell wave height (Hsw) and swell wave period (Tsw) for 1200 h of 25 January, 25 April, 25 July and 25 October 2000 are shown in Figures 3-7 respectively. Figure 3 (25 January 2000, 1200 hrs) shows that, Hs varied from 1 to 2.0 m, with a gradual increase from north to south of North Indian Ocean. The mean wave direction followed the prevailing wind pattern. The Tc, Hsw and Tsw as shown in Figure 3 show spatial variations ranging from 6 to 9 s, 1.0 to 1.8 m and 8 to 9 s respectively. It may be noted that there is a marginal variation between the Hs and Hsw, about 0.2 m. The same is the case between Tc and Tsw.

The spatial distribution of Hs, Tc, mean wave direction, Hsw and Tsw for 25 April 2000, 1200 hrs are plotted in Figure 4. Hs varied from about 1.0 to 2.0 m in the Arabian Sea and 0.4 to 2.0 m in the Bay of Bengal. The Hs maxima of 2.0 m was seen in the south-central region of North Indian Ocean. Tc varied between 6 and 12 s in the Arabian Sea, whereas it varied from 7 to 10 s in the Bay of Bengal. The mean wave directions more or less agree with the prevailing wind pattern over the Arabian Sea (north-westerly) and similar is the wave direction pattern in the Bay of Bengal. Hsw ranged between 1.0 and 1.8 m in the Arabian Sea, whereas it varied from 0.4 to 1.6 m in the Bay of Bengal. Tsw varied from 8 to 9 s in the Arabian Sea and 6 to 9 s in the Bay of Bengal respectively.

The high wind and wave conditions are observed during the southwest monsoon indicating the rough weather season. However, on 25 July 2000 the sea-state was moderate with maximum Hs about 2.4 m in southwest Arabian Sea. In the Arabian Sea (Figure 5). Hs varied from 1.2 to 2.4 m with Tc ranging from 6 to 11 s. Hsw varied from 1.0 to 2.0 m with Tsw 8 to 9 s. However, in the Bay of Bengal, Hs was lower (0.6 to 1.6 m) as compared to the Arabian Sea. Tc varied from 5 to 9 s, Hsw from 0.6 to 1.4 m and Tsw from 6 to 8 s.

From this hindcast case study of July 2000, four selected sample wave spectra of 10 July 2000 (1200 hrs) from four selected locations in the Indian Seas(Location 1: 0°N, 90°E; Location 2: 8°S, 55° E; Location 3: 12°S, 67°E; Location 4: 15°N, 90°E) are shown in Figure 6. The sample plots of 1D (frequency) spectra for 10 July 2000 (1200 h) as shown in Figure 6 reveal multi-peaked spectral characteristics indicating the presence of a predominant wind-sea and minor swell peak. Although

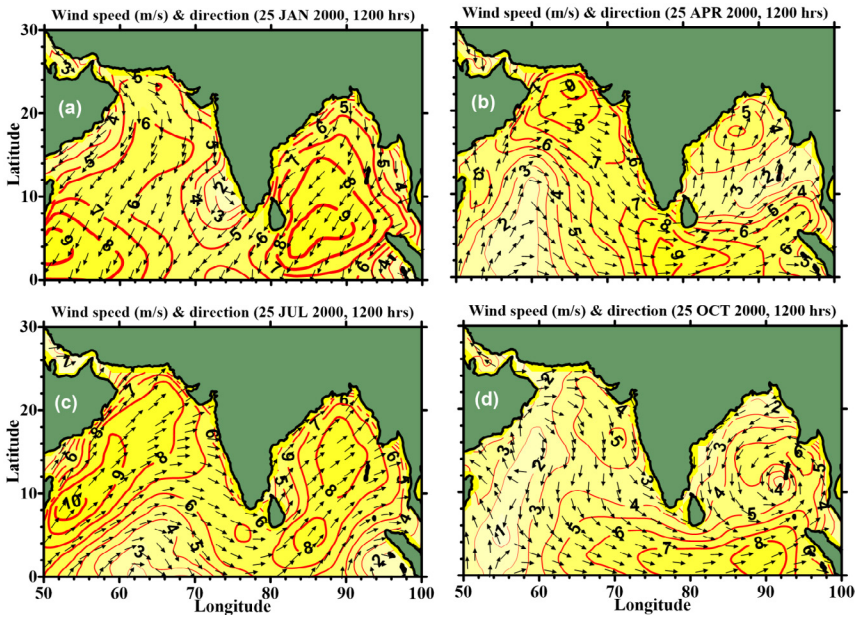

Figure 2: Input wind field (ERA-40), wind speed (m/s) and direction (arrows) for wave hindcast using WWIII for the North Indian Ocean.

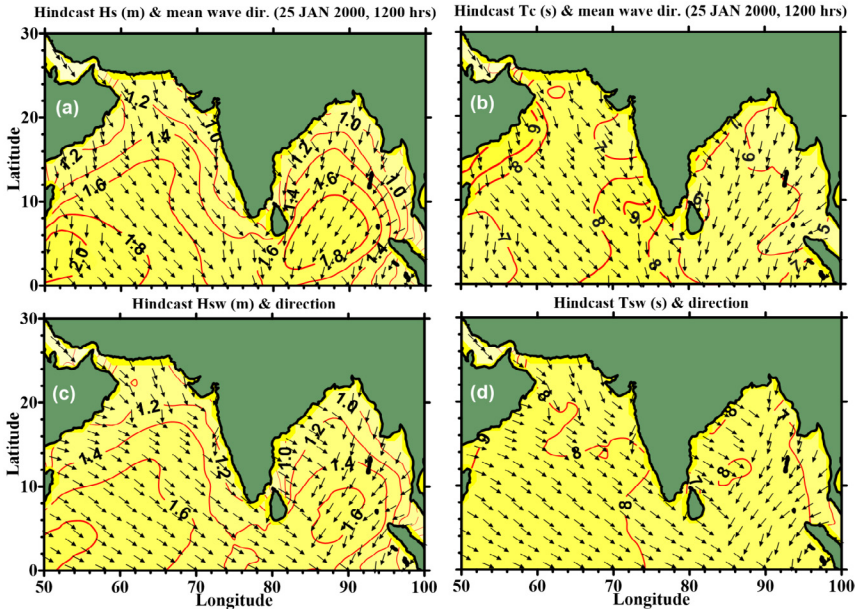

Figure 3: WWIII hindcast wave fields using ERA-40 analysed winds, 25 January 2000, 1200 hrs.

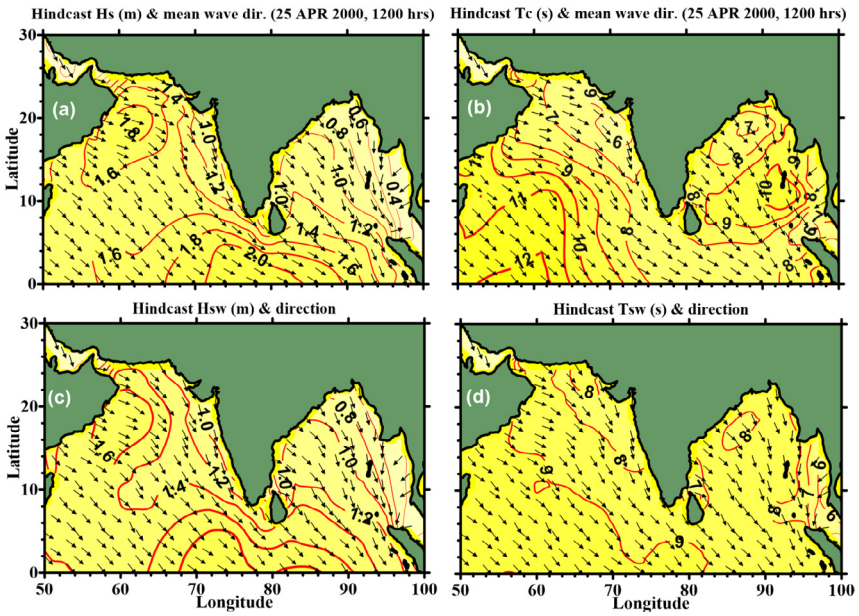

Figure 4: WWIII hindcast wave fields using ERA-40 analysed winds, 25 April 2000, 1200 hrs.

the winds during July (southwest monsoon) are strong and steady, the major wave generating areas can be more than one due to which swells can propagate from the south. Such spectra can also be generated due to time varying winds over a large area. The frequency spectrum of 10 July 2000, 1200 h belong to the active monsoon phase with minor swell components.

The hindcast wave parameters for 25 October 2000, 1200 hrs as shown in Figure 7 indicate low wave activity with a lower range of spatial variability, Hs being higher in southeaster part of North Indian Ocean. The Hs varied from 1.0 to 1.8 m in the Arabian Sea, while in the Bay of Bengal it ranged from 0.6 to 2.0 m. The Tc varied from 8 to 11 s in the Arabian Sea and from 5 to 12 s in the Bay of Bengal. The hindcast Hsw ranged from 1.0 to 1.6 m in the Arabian Sea while it varied from 0.6 to 1.6 m in the Bay of Bengal. In the Arabian Sea, Ts varied from 9 to 10 s; and in the Bay of Bengal, it ranged from 6 to 10 s.

In this case study involving four months of wave hindcasts using ERA-40 winds could be a consolidation of typical case studies mimicking a general pattern of wind and wave variability in association with commonly occurring local and temporal variabilities in the North Indian Ocean during pre-monsoon, southwest monsoon, northeast monsoon and post-monsoon periods. The model performances and their ranges of hindcast wave variabilities in space and time for the four

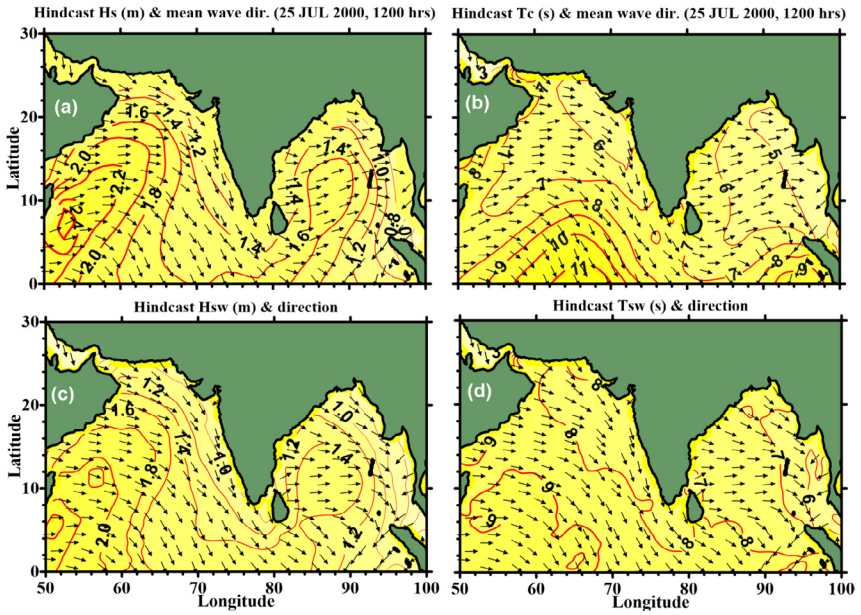

Figure 5: WWIII hindcast wave fields using ERA-40 analysed winds, 25 July 2000, 1200 hrs.

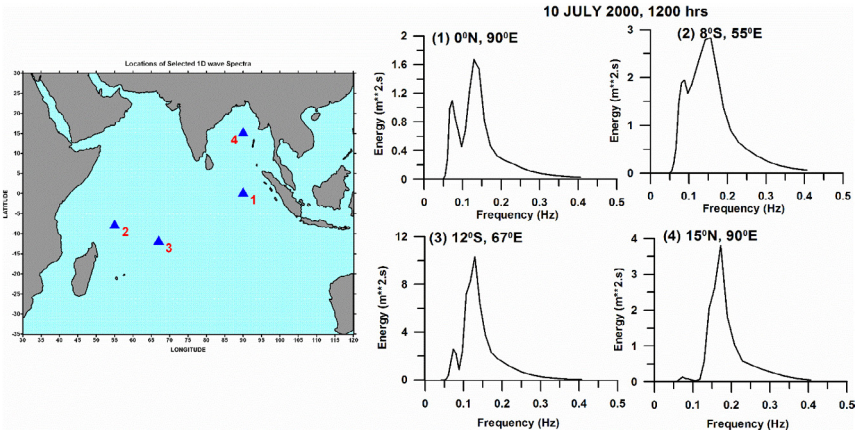

Figure 6: Predicted 1D wave spectra for four selected locations (Indian Seas) using ERA-40 winds.

selected months (year 2000) were useful and form as the background information while validating WWIII using *in situ* measurements.

Wave Hindcasts - Case-II: July 2008 and January 2009

In this case study, the QuikSCAT/NCEP blended winds (July 2008 and January 2009) are used as input to force the WWIII model. The spatial distribution of input wind fields for the North Indian Ocean for the day (25th, 1200 hrs) are shown for the months of July 2008 and January 2009 respectively in Figure 8. Figure 8a shows the wind speed and direction for the 25 July 2008, 1200 hrs, which is predominantly southwesterly. However, the winds turn westerly near the coast and turn further around northwesterly very close to the coast while approaching the landmass (Western Ghats). This is a consistent and regular feature of southwest winds which may vary marginally from north to south along the west coast of India. Figure 8b clearly depicts the very high wind speeds which prevail during July, being the peak of southwest monsoon. Compared with July 2008, the wind speeds were low for 25 January 2009, 1200 hrs (Figure 8), being the fair weather period. January is the peak of northeast monsoon and on 25 January 2009, 1200 hrs, the winds ranged from 2 to 8 m/s which were predominantly northeasterly. The spatial distributions or the contour plots of hindcast Hs, mean wave direction, Tc, Hsw and Tsw for 25 July 2008, 1200 hrs and 25 January 2009, 1200 hrs are shown in Figures 9 and 10 respectively.

The contour plots showing spatial variability of wave parameters for 25 July 2008, 1200 hrs reveal about the usually occurring high wave activity during the active or peak southwest monsoon period during which Hs reaches around 5 to 6 m off the Somali coast and 3 m waves are noticed in the Bay. As shown in Figure 9, the Hs varied from 1.5 to 5.0 m in the Arabian Sea, while in the Bay of Bengal it ranged from 1.5 to 3.0 m, maximum being in southern Bay.

The Tc varied from 6 to 10 s in the Arabian Sea and from 5 to 8 s in the Bay of Bengal which is consistent with the corresponding Hs fields

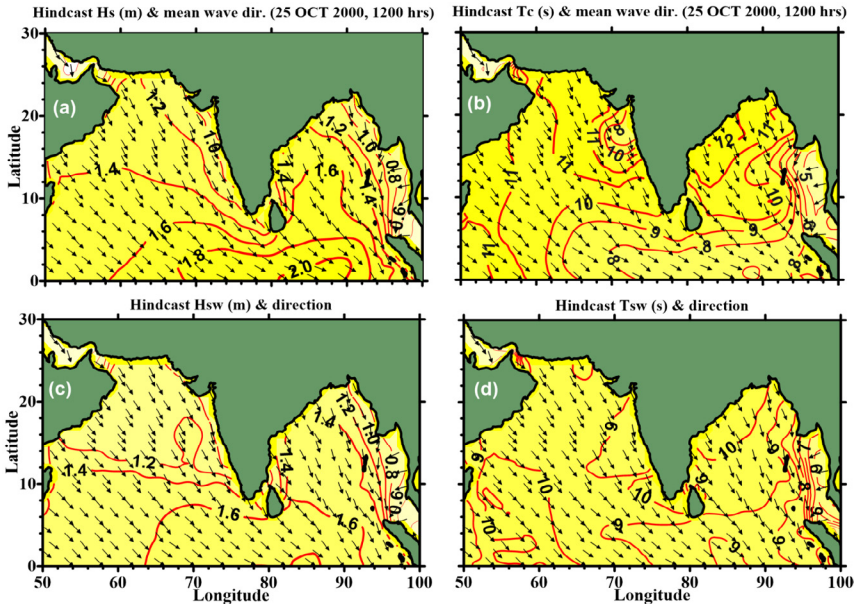

Figure 7: WWIII hindcast wave fields using ERA-40 analysed winds, 25 October 2000, 1200 hrs.

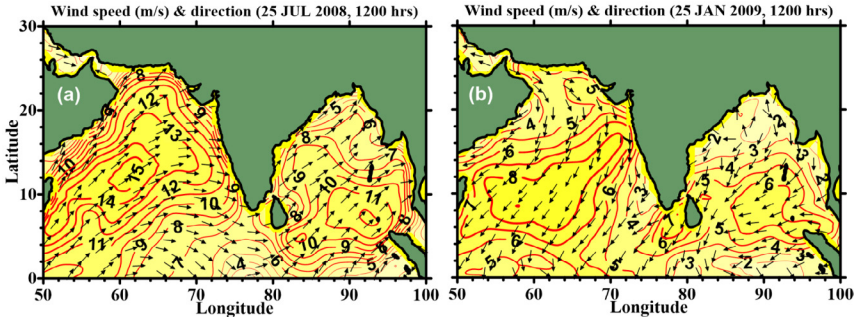

Figure 8: Input wind field (QuikSCAT/NCEP blended), wind speed (m/s) and direction (arrows) for wave hindcast using WWIII for the North Indian Ocean.

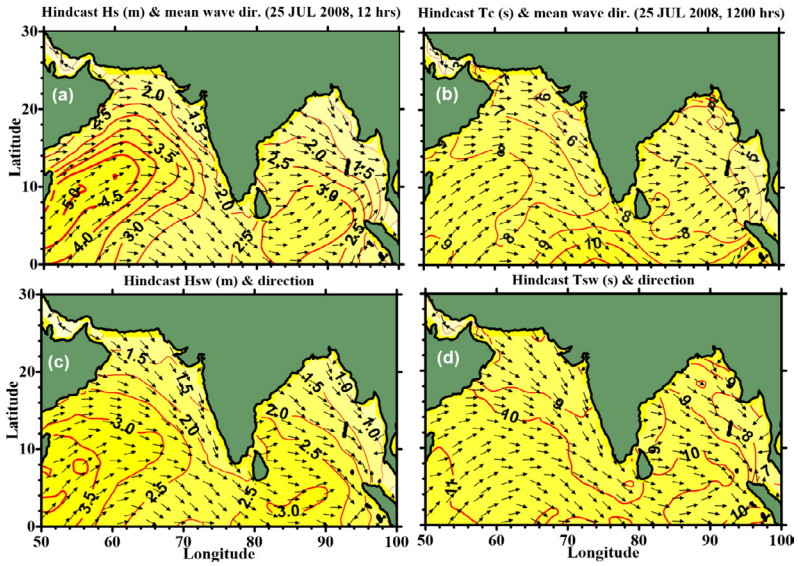

Figure 9: WWIII hindcast wave fields using QuikSCAT/NCEPblended winds, 25 July 2008, 1200 hrs.

during summer monsoon. Similarly, the hindcast Hsw varied from 1.5 to 3.5 m in the Arabian Sea, and in Bay of Bengal, it varied from 1.0 to 3.0 m. In the Arabian Sea, Tsw varied from 9 to 11 s, while in the Bay of Bengal it ranged from 7 to 10 s. The swell wave field indicates that the local wave activity was strong enough to generate high wind-seas up to 5.0 m in the Arabian Sea while the swells generated in the Southern Ocean co-existed.

For the month of January 2009, the hindcast Hs varied from 1.4 to 2.0 m in the Arabian Sea and 0.8 to 1.6 m in the Bay of Bengal for 25 January 2009, 1200 hrs as shown in Figure 10. Tc varied between 5 to 10 s in the Bay of Bengal, whereas it varied from 8 to 9 s in the Arabian Sea. The hindcast Hsw varied from 1.4 to 2.0 m in the Arabian Sea and 1.2 to 1.6 m in the Bay of Bengal. Tsw was around 9 s in the Arabian Sea, while it varied from 6 to 10 s in the Bay of Bengal. This is a typical example of wind and wave variability during January 2009 (peak of northeast monsoon) during which the mean wave directions as well as the swell directions were around north (± 45^0). Figure 10 reveals that although the strength of the wind was reasonably high because high wave activity, which generally occur in January during northeast monsoon, swell waves were equally predominant due to time varying north-easterly winds.

Besides the sample spatial plots as shown in Figure 10 for the month of January 2009, the time-series of few selected wind and wave parameters (Location 2: 8°S, 55°E) have been shown in Figure 11. The time-series of wind and hindcast wave parameters at the selected location from 01-31 January 2009 as shown in Figure 11 indicate moderate to high wind and wave variability (winter monsoon) with speeds ranging between 3 to 9 m/s and Hs between 0.7 to 2.2 m. The

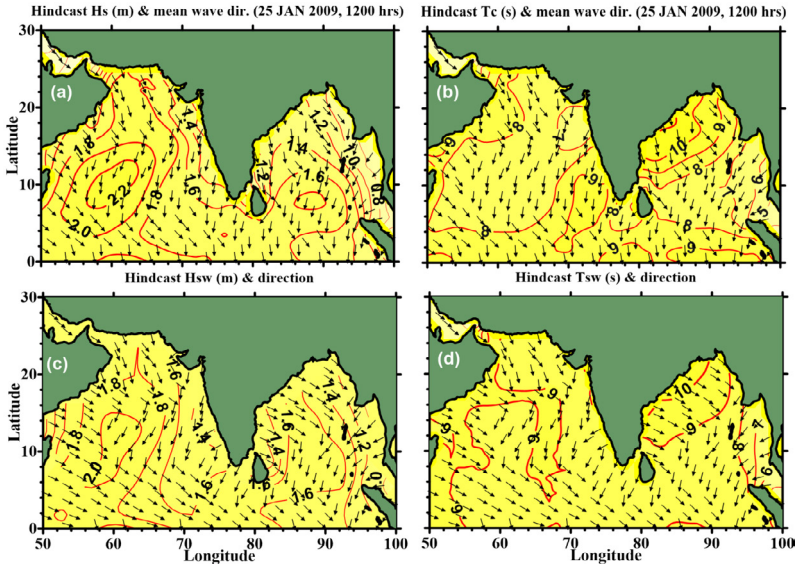

Figure 10: WWIII hindcast wave fields using QuikSCAT/NCEP blended winds, 25 January 2009, 1200 hrs.

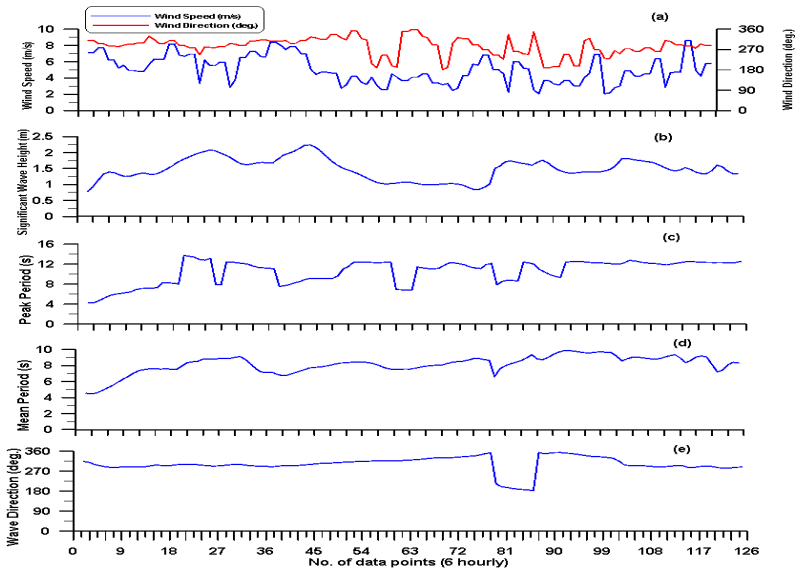

Figure 11: Time series of wind and wave parameters at selected location (55°E, 8°S), 01-31 January 2009 (a) Wind speed (m/s) & direction (deg.), (b) Significant wave height (m), (c) Peak Period (s), (d) Mean Period (s) and (e) Wave direction (deg.).

hindcast time-series of peak wave period and Tc reveal the changing sea-state conditions (transition between wind-seas and swells) depending on the coupling strength of wind and waves. The mean wave direction seems to be more or less steady as compared to the wind as shown in Figure 11 and in agreement with the prevailing wind pattern.

Validation of WWIII in the Arabian Sea and Bay of Bengal

The observed met-ocean parameters such as Hs and Tc of NDBP being executed by NIOT for the buoys named DS1, DS2, DS3, DS4, SW1, SW4, SW5, SW6, OB10 all located in deep waters have been co-located and interpolated in space and time for the comparisons with WWIII model outputs. The buoy locations in the Arabian Sea and Bay of Bengal utilised in this study is as shown in Figure 1. A detailed statistical error analysis is performed for each dataset to evaluate the model performance. Figures 12-15 shows the comparison between the observed and predicted wave parameters (Hs and Tc) at 6 hourly intervals for the periods of 01-31 January, 01-30 April, 01-31 July and 01-31 October 2000 respectively. The statistical estimates for the validation of wave model (WWIII) with buoy measurements in the

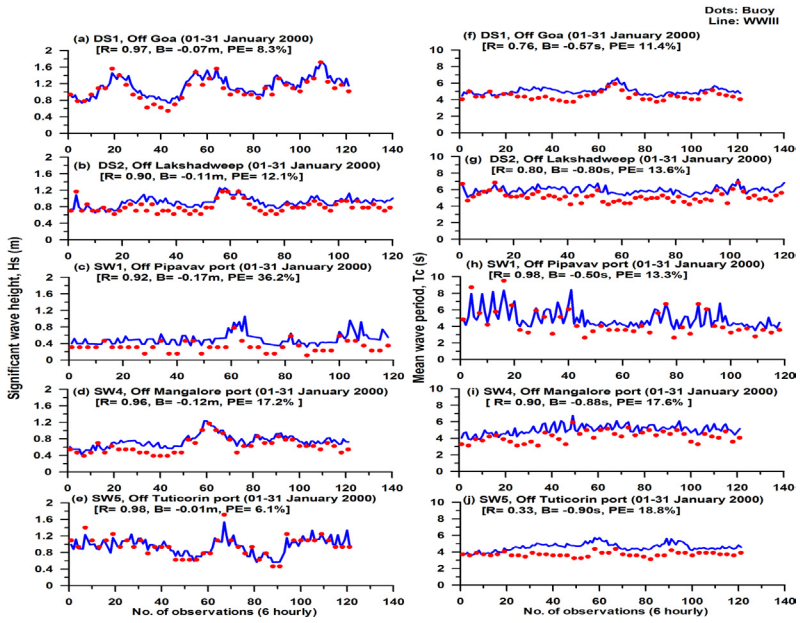

Figure 12: Comparison between the observed (NIOT buoys) and predicted wave parameters at 6 hourly intervals for the period January 2000 using ERA-40 winds.

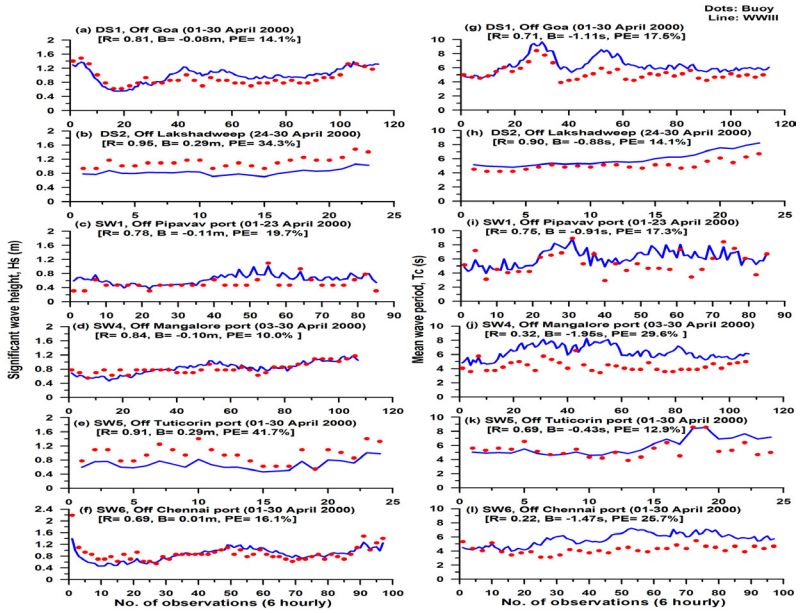

Figure 13: Comparison between the observed (NIOT buoys) and predicted wave parameters at 6 hourly intervals for the period April 2000 using ERA-40 winds.

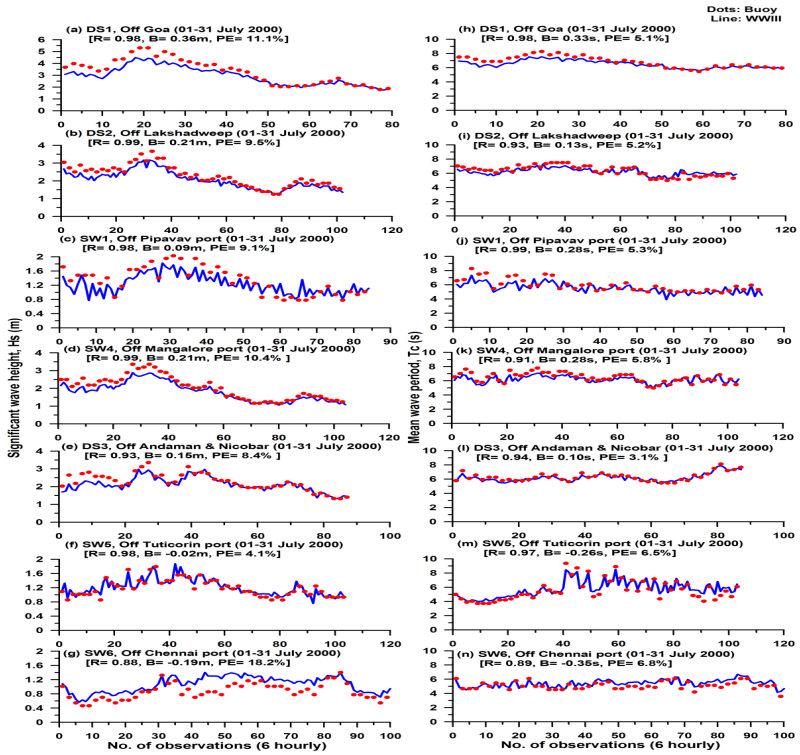

Figure 14: Comparison between the observed (NIOT buoys) and predicted wave parameters at 6 hourly intervals for the period July 2000 using ERA-40 winds.

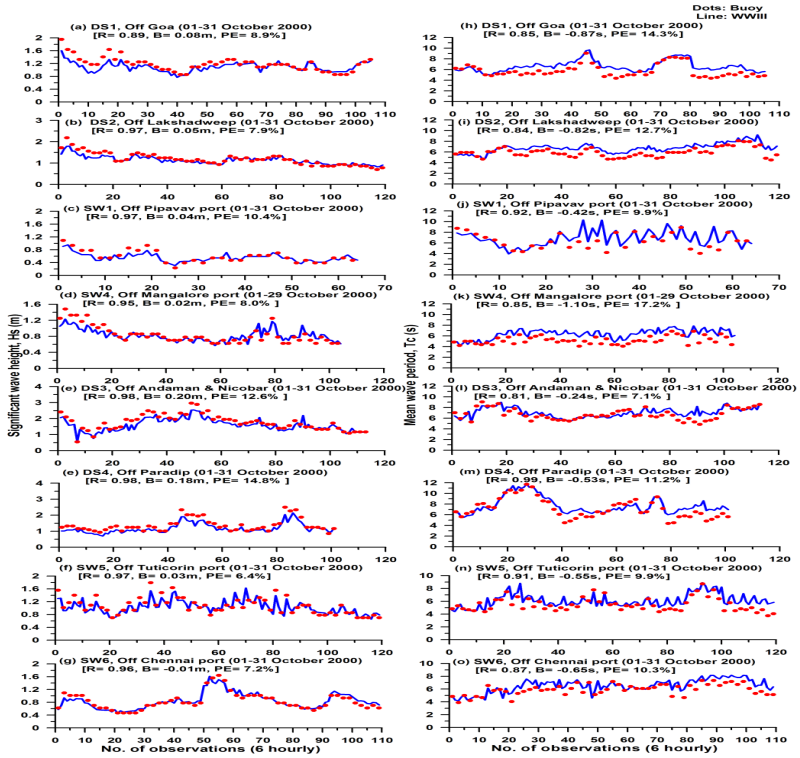

Figure 15: Comparison between the observed (NIOT buoys) and predicted wave parameters at 6 hourly intervals for the period October 2000 using ERA-40 winds.

Indian Seas during January 2000 are shown in Table 2. In Figure 12, the WWIII model outputs (continuous line in blue) are compared with measurements from five buoy (solid circles in red color) locations such as DS1, DS2, SW1, SW4 and SW5 for the period 01-31 January 2000. The length of the time-series or the number of data points plotted for comparison between the model and buoy observations may vary due to missing buoy data.

In general, the model predicted parameters Hs and Tc as shown in Figure 12 reveal very good correlation with the observations in most cases. Korres et al. [33] and Montoya et al. [37] have reported that, WWIII performed well showing best statistical estimates with the observedwave parameters such as Hs and Tc for the Mediterranean Sea and Gulf of Mexico respectively. In this case, the buoy observations such as DS1, DS2, SW1 and SW4 in the Arabian Sea *versus* the model hindcasts for Hs indicate correlation coefficients of the order 0.90 to 0.97, while in theBay of Bengal, it is 0.98 for SW5. The mean as well as range of Hs, both for buoy measurements and the model predictions are well comparable. However, in case of Tc the mean values of buoys and hindcasts deviates up to 1.5 s and the ranges too deviated up to 1.1 s. The lower values of SI (0.01 to 0.10) for DS1, DS2, SW1, SW4 and SW5 respectively for Hs indicate better fits between the model and measurements. At all the buoy locations considered, Hs shows negative bias for DS1, DS2, SW1, SW4 and SW5 respectively which indicate marginal overestimation by the wave model (WWIII) hindcasts. The RMSE is low in all cases, which reveal a better agreement between the model and observations. The PE for Hs is lesser than 18% in most cases except one case (SW1), where it is higher (36.2%), obviously due to the prevailing low wind and wave activity period. It is also noted that the analysed winds during such low wind events generally do not reflect the real-world conditions. The higher values of MPI for the buoys (DS1, DS2, SW1, SW4 and SW5) reveal considerably a good model performance (WWIII) with the use of NIOT buoy measurements.

The predicted Tc and the measurements show correlation coefficients in the range 0.76 to 0.98 in the Arabian Sea, which agree with the earlier results reported by Remya et al. However, the correlation coefficient is low (R=0.33) in case of SW5, in the Bay of Bengal. Values of SI are lower in most cases (DS1, DS2, SW1, SW4 and SW5) which indicate still a better comparison between the observed and hindcast Tc. The values of B are negative throughout which indicates that predicted values of Tc by WWIII are higher with maximum deviation being up to 1 s. The estimated RMSE values are in the range 0.43 to 1.00 (for DS1, DS2, SW1, SW4 and SW5 buoys). The PE considering all buoy locations remained within 20% for Tc, although it was a fair-weather season (January 2000). MPI is in the range 0.80 to 0.90 in the Arabian Sea and 0.73 for SW5 in the Bay of Bengal.

Figure 13 shows the comparison between the observed and predicted wave parameters (Hs and Tc) of WWIII for the period 01-30 April 2000. Here, the model outputs are validated for six buoy locations such as DS1, DS2, SW1, SW4, SW5 and SW6. Compared with the previous study of January 2000 (five buoys), here we have an additional buoy SW6 for WWIII validation. The computed statistical estimates for the hindcast parameters Hs and Tc and the buoy measurements during April 2000 are shown in Table 3. In the Arabian Sea, the WWIII hindcasts and the measurements of buoys DS1, DS2, SW1 and SW4 shows correlation coefficients in the range 0.78 to 0.95 for Hs, while in the Bay of Bengal, model hindcasts against SW5 and SW6 buoy measurements show correlation coefficients of 0.91 and 0.69 respectively for Hs. It is noted that SI is low in all cases indicating a better fit between measured and model Hs. Bias is negative for DS1, SW1 and SW4 buoys against model hindcasts. Positive bias is observed for DS2, SW5 and SW6 which signifies modelcomputed Hs are marginally higher compared to buoy observations. The PE for Hs

2.1. Significant wave height (Hs in m)						
Sl. No.	**Statistical estimates**	**Arabian Sea**				**Bay of Bengal**
		DS1	**DS2**	**SW1**	**SW4**	**SW5**
1.	Mean (Buoy)	1.1	0.8	0.3	0.6	1.0
2.	Range (Buoy)	0.5 - 1.7	0.6 – 1.2	0.1 – 0.9	0.3 – 1.2	0.5 – 1.7
3.	Mean (WWIII)	1.0	0.9	0.5	0.7	0.9
4.	Range (WWIII)	0.7 – 1.7	0.6 – 1.2	0.3 – 1.1	0.4 – 1.2	0.6 – 1.5
5.	R	0.97	0.90	0.92	0.96	0.98
6.	SI	0.01	0.02	0.10	0.03	0.01
7.	B	-0.07	-0.11	-0.17	-0.12	-0.01
8.	RMSE	0.01	0.01	0.03	0.02	0.01
9.	PE	8.3	12.1	36.2	17.2	6.1
10.	MPI	0.99	0.98	0.90	0.97	0.99
2.2. Mean wave period (Tc in s)						
1.	Mean (Buoy)	4.5	5.1	4.4	4.2	3.7
2.	Range (Buoy)	3.6 – 6.2	4.2 – 6.9	2.6 – 9.5	3.0 – 5.9	3.1 – 4.4
3.	Mean (WWIII)	5.0	5.9	4.9	5.1	4.6
4.	Range (WWIII)	4.3 – 6.6	5.1 – 7.3	3.5 – 8.4	3.8 – 6.7	3.6 – 5.7
5.	R	0.76	0.80	0.98	0.90	0.33
6.	SI	0.10	0.15	0.11	0.20	0.27
7.	B	-0.57	-0.80	-0.50	-0.88	-0.90
8.	RMSE	0.43	0.75	0.47	0.85	1.00
9.	PE	11.4	13.6	13.3	17.6	18.8
10.	MPI	0.90	0.85	0.89	0.80	0.73

***R:** Correlation Coefficient, **SI:** Scatter Index, **B:** Bias, **RMSE:** Root Mean Square Error, **PE:** Percentage Error & **MPI:** Model Performance Index.*

Table 2: Statistics of the comparison of WWIII model wave parameters with NIOT buoy measurements in the Arabian Sea and Bay of Bengal during January 2000 using ERA-40 winds as shown in figure 12.

Sl. No.	Statistical estimates	Arabian Sea				Bay of Bengal	
		DS1	DS2	SW1	SW4	SW5	SW6
3.1. Significant wave height (Hs in m)							
1.	Mean (Buoy)	0.9	1.1	0.5	0.8	1.0	0.9
2.	Range (Buoy)	0.6 – 1.5	0.9 – 1.5	0.3 – 1.1	0.5 – 1.2	0.5 – 1.4	0.5 – 2.2
3.	Mean (WWIII)	1.0	0.8	0.6	0.9	0.7	0.8
4.	Range (WWIII)	0.5 – 1.4	0.7 – 1.1	0.4 – 1.0	0.5 – 1.2	0.5 – 1.0	0.5 – 1.4
5.	R	0.81	0.95	0.78	0.84	0.91	0.69
6.	SI	0.03	0.08	0.04	0.01	0.10	0.03
7.	B	-0.08	0.29	-0.11	-0.10	0.29	0.01
8.	RMSE	0.02	0.09	0.02	0.01	0.10	0.03
9.	PE	14.1	34.3	19.7	10.0	41.7	16.1
10.	MPI	0.97	0.92	0.96	0.99	0.90	0.97
3.2. Mean wave period (Tc in s)							
1.	Mean (Buoy)	5.2	5.0	5.3	4.4	5.4	4.2
2.	Range (Buoy)	3.9 – 9.4	4.2 – 6.7	3.0 – 8.9	3.4 – 6.6	3.9 – 8.6	3.1 – 6.4
3.	Mean (WWIII)	6.3	5.9	6.2	6.4	5.9	5.7
4.	Range (WWIII)	4.6 – 9.7	4.8 – 8.2	4.0 – 8.9	4.5 – 8.3	4.6 – 8.5	4.0 – 7.2
5.	R	0.71	0.90	0.75	0.32	0.69	0.22
6.	SI	0.37	0.21	0.31	1.07	0.20	0.71
7.	B	-1.11	-0.88	-0.91	-1.95	-0.43	-1.47
8.	RMSE	1.93	1.06	1.66	4.73	1.07	3.02
9.	PE	17.5	14.1	17.3	29.6	12.9	25.7
10.	MPI	0.63	0.79	0.69	0.17	0.80	0.29

***R:** Correlation Coefficient, **SI:** Scatter Index, **B:** Bias, **RMSE:** Root Mean Square Error, **PE:** Percentage Error & **MPI:** Model Performance Index.*

Table 3: Statistics of the comparison of WWIII model wave parameters with NIOT buoy measurements in the Arabian Sea and Bay of Bengal during April 2000 using ERA-40 winds as shown in figure 13.

is within 20% for most buoys, while it is considerably higher forDS2 (34.3%) and SW5 (41.7%) where the model could not show a better prediction for Hs, at these buoy locations. The MPI for the Arabian Sea buoys DS1, DS2, SW1 and SW4 varied from 0.92 to 0.99. In Bay of Bengal, the MPI is equally high such as 0.90 and 0.97 for SW5 and SW6 buoy locations respectively.

The Tc also shows reasonably good correlations in the Arabian Sea (0.71 to 0.90), except in one case i.e. 0.32 for SW4, which is quite low. Tc also shows poor correlation of 0.22 for SW6 location in the Bay of Bengal while it shows better correlation of 0.69 for SW5 in the Bay of Bengal. The low correlation coefficient in few cases can be assigned to the fair weather season (April 2000) which experiences low wind conditions, i.e. inaccurately driven by the low quality input winds. Bias is negative throughout which are in the range of approximately -0.5 to -2.0. RMSE varied in the range 1.06 to 1.93 in all cases, except for two buoysSW4 and SW6, which reveal higher values showing large deviations (4.73 and 3.02). The PE remained within 20% for most cases except in two cases where it is higher (SW4:29.6% and SW6: 25.7%). The MPI is lower in two cases; 0.17 for SW4 in the Arabian Sea and 0.29 for SW6 in the Bay of Bengal which is mainly due to the low wind and wave conditions during fair weather season, which can be, attributed to inaccurate input wind fields.

Figure 14 shows the comparison between the observed and predicted wave parameters (Hs and Tc) at 6 hourly intervals for the period 01-31 July 2000. Here, the WWIII model outputs are validated for seven buoy locations such as DS1, DS2, SW1, SW4, DS3, SW5 and SW6. The statistics of the comparison of WWIII hindcast wave parameters (Hs and Tc) with buoy measurements in the Indian Seas during July 2000 is shown in Table 4. The model predicted parameters as shown in Figure 14 shows reasonably strong correlation with the observations. Similar results have been reported by Samiksha et al., for the Indian Ocean region. The observed and hindcast mean and ranges for Hs and Ts compare well with each other. In the Arabian Sea and Bay of Bengal, the buoys versus the model hindcasts shows a very strong correlation for Hs. The SI values are representative of a better fit between the model and buoy for Hs. PE is lower in all cases (<12%) except in one case SW6, where it is 18.2%. The MPI was equally strong enough in both Arabian Sea and Bay of Bengal.

Similar to Hs; Tc also shows a very strong correlation between the buoys and WWIII hindcasts in the Arabian Sea and Bay of Bengal. Bias is positive in most cases; while it is negative for SW5 (-0.26) and (-0.35). RMSE varied in the range 0.05 to 0.20 for the buoys considered which shows good agreement between the hindcast and observed Tc. The PE of WWIII is very less (<7%) and highly promising for all buoys in the Indian seas. MPI is also considerably high such as 0.96 to 0.98 in the Arabian Sea and 0.96 to 0.99 in the Bay of Bengal indicating strong agreement between the model and measured Tc.

Figure 15 shows the comparison between the observed and hindcast wave parameters (Hs and Tc) at 6 hourly intervals for the period 01-31 October 2000. The WWIII hindcast wave parameters are validated for eight buoy locations such as DS1, DS2, SW1, SW4, DS3, DS4, SW5 and SW6. Statistical estimates on the comparison between WWIII model predicted wave parameters with buoy measurements in the Indian Seas during October 2000 is shown in Table 5. Here the hindcast parameters as shown in Figure 15 reveal considerably higher correlations with the buoy observations. Similar degree of comparisons between WWIII and corresponding wave measurements are reported for the north Indian Ocean by Samiksha et al. [38]. Surprisingly, the difference in the hindcast and observed mean for Hs during October 2000 and the ranges at all the buoy locations considered are well within 0.1 m and 0.4 m respectively, although October is the post-monsoon month. However, in this case, the buoys in the Arabian Sea shows

4.1. Significant wave height (Hs in m)								
Sl. No.	**Statistical estimates**	**Arabian Sea**				**Bay of Bengal**		
		DS1	**DS2**	**SW1**	**SW4**	**DS3**	**SW5**	**SW6**
1.	Mean (Buoy)	3.3	2.3	1.3	2.0	2.3	1.2	0.9
2.	Range (Buoy)	1.8 – 5.5	1.2 – 3.7	0.7 – 2.1	1.1 – 3.3	1.2 – 3.5	0.7 – 2.0	0.4 – 1.4
3.	Mean (WWIII)	2.9	2.0	1.2	1.8	2.1	1.2	1.1
4.	Range (WWIII)	1.7 – 4.5	1.2 – 3.2	0.8 – 1.8	1.1 – 2.9	1.3 – 3.0	0.8 – 1.9	0.6 – 1.4
5.	R	0.98	0.99	0.98	0.99	0.93	0.98	0.88
6.	SI	0.07	0.03	0.02	0.03	0.03	0.01	0.05
7.	B	0.36	0.21	0.09	0.21	0.15	-0.02	-0.19
8.	RMSE	0.23	0.06	0.02	0.06	0.06	0.01	0.05
9.	PE	11.1	9.5	9.1	10.4	8.4	4.1	18.2
10.	MPI	0.94	0.97	0.98	0.98	0.97	0.99	0.96
4.2. Mean wave period (Tc in s)								
1.	Mean (Buoy)	6.8	6.3	5.8	6.5	6.3	5.5	5.1
2.	Range (Buoy)	5.5 – 8.3	5.0 – 8.0	3.6 – 8.3	5.0 – 7.8	5.1 – 8.1	3.7 – 9.4	3.4 – 6.4
3.	Mean (WWIII)	6.5	6.2	5.5	6.2	6.2	5.8	5.4
4.	Range (WWIII)	5.6 – 7.5	5.3 – 7.3	3.9 – 7.3	5.0 – 7.1	5.4 – 7.9	4.0 – 8.5	4.2 – 6.7
5.	R	0.98	0.93	0.99	0.91	0.94	0.97	0.89
6.	SI	0.03	0.02	0.03	0.03	0.01	0.04	0.04
7.	B	0.33	0.13	0.28	0.28	0.10	-0.26	-0.35
8.	RMSE	0.17	0.14	0.17	0.18	0.05	0.20	0.18
9.	PE	5.1	5.2	5.3	5.8	3.1	6.5	6.8
10.	MPI	0.97	0.98	0.97	0.96	0.99	0.96	0.97
***R:** Correlation Coefficient, **SI:** Scatter Index, **B:** Bias, **RMSE:** Root Mean Square Error, **PE:** Percentage Error & **MPI:** Model Performance Index.*								

Table 4: Statistics of the comparison of WWIII model wave parameters with NIOT buoy measurements in the Arabian Sea and Bay of Bengal during July 2000 using ERA-40 winds as shown in figure 14.

5.1. Significant wave height (Hs in m)									
Sl. No.	**Statistical estimates**	**Arabian Sea**				**Bay of Bengal**			
		DS1	**DS2**	**SW1**	**SW4**	**DS3**	**DS4**	**SW5**	**SW6**
1.	Mean (Buoy)	1.2	1.3	0.6	0.9	1.8	1.3	1.1	0.8
2.	Range (Buoy)	0.8 – 1.9	0.7 – 2.2	0.2 – 1.2	0.5 – 1.5	0.5 – 3.0	0.8 – 2.6	0.5 – 1.8	0.5 – 1.8
3.	Mean (WWIII)	1.0	1.1	0.5	0.8	1.6	1.2	1.0	0.9
4.	Range (WWIII)	0.8 – 1.6	0.8 – 1.8	0.3 – 0.9	0.6 – 1.2	0.6 – 2.5	0.7 – 2.1	0.6 – 1.6	0.5 – 1.6
5.	R	0.89	0.97	0.97	0.95	0.98	0.98	0.97	0.96
6.	SI	0.01	0.02	0.01	0.02	0.03	0.03	0.01	0.01
7.	B	0.08	0.05	0.04	0.02	0.20	0.18	0.03	-0.01
8.	RMSE	0.02	0.02	0.01	0.01	0.06	0.04	0.01	0.01
9.	PE	8.9	7.9	10.4	8.0	12.6	14.8	6.4	7.2
10.	MPI	0.98	0.99	0.98	0.99	0.97	0.97	0.99	0.98
5.2. Mean wave period (Tc in s)									
1.	Mean (Buoy)	5.7	5.9	6.4	5.2	6.8	7.2	5.6	5.9
2.	Range (Buoy)	4.4 – 9.2	4.5 – 8.6	3.7 – 10.5	3.9 – 7.0	4.8 – 9.1	4.4 – 11.7	3.7 – 8.7	3.6 – 7.3
3.	Mean (WWIII)	6.6	6.8	6.8	6.3	7.0	7.7	6.1	6.5
4.	Range (WWIII)	5.0 – 9.7	4.7 – 9.2	3.9 – 10.3	4.3 – 7.9	5.3 – 9.0	5.5 – 11.7	4.4 – 8.9	4.2 – 8.2
5.	R	0.85	0.84	0.92	0.85	0.81	0.99	0.91	0.87
6.	SI	0.20	0.15	0.09	0.27	0.06	0.14	0.09	0.12
7.	B	-0.87	-0.82	-0.42	-1.10	-0.24	-0.53	-0.55	-0.65
8.	RMSE	1.14	0.90	0.60	1.41	0.39	1.00	0.52	0.69
9.	PE	14.3	12.7	9.9	17.2	7.1	11.2	9.9	10.3
10.	MPI	0.80	0.85	0.91	0.73	0.94	0.86	0.91	0.88
***R:** Correlation Coefficient, **SI:** Scatter Index, **B:** Bias, **RMSE:** Root Mean Square Error, **PE:** Percentage Error & **MPI:** Model Performance Index.*									

Table 5: Statistics of the comparison of WWIII model wave parameters with NIOT buoy measurements in the Arabian Sea and Bay of Bengal during October 2000 using ERA-40 winds as shown in figure 15.

considerably good correlations with the model hindcasts, while in the Bay of Bengal in spite of variable windsthe buoys DS3, DS4, SW5 and SW6 show still higher correlations of the order 0.96 to 0.98 with hindcast Hs. The value of SI is 0.01, same for four different wave buoys such as DS1, SW1, SW5, and SW6. It is 0.02 for DS2 and SW4, 0.03 for DS3 and DS4, which indicate significant fit between the model and observed Hs. It may be noted here that, on 25th October 2000 a tropical depression developed in central Bay of Bengal and dissipated

on 28th and its effect is clearly observed by DS4 buoy as shown in Figure 15. The PE estimates are <15% in all cases considered. The values of MPI are high enough (near to 1.0) for all the buoys considered which indicate minimum uncertainty in model predictions.

The hindcast Tc also shows good correlation (R> 0.8) in the Arabian Sea and Bay of Bengalagainst measurements. SI varied in the range 0.06 to 0.27; which are lower indicating a better fit. Bias is negative throughout for all buoys considered with PE < 18 %. The high values of MPI and lower values of PE clearly indicates that the model could reasonably reproduce the wave periods at the buoy locations during the post monsoon month of October 2000 with low uncertainty.

Figure 16 shows the comparison between the buoy OB10 and the hindcast wave parameters (Hs and Tc) at 6 hourly intervals for the period 01-31 January 2009. The estimated statistics for the comparison of WWIII model wave parameters with the buoy measurements in the Bay of Bengal is shown in Table 6. The WWIII model predicted parameters (both Hs and Tc) as shown in Figure 16 show significant correlation with the observations. In another recent study, Sabique et al. [39] have validated MIKE21 SW model [40] results with OB10 buoy measurements for the period from October 2008 to August 2009. Their study (comparisons between model and buoy) reports: R value 0.93, bias of 0.11, RMSE (0.30) and SI (0.19) for Hs and R value (0.67), bias of -0.81, RMSE (1.2) and SI (0.21) respectively for Tc. Here, the estimated means and ranges of Hs for the buoy and WWIII hindcasts are wellin agreement with each other. The buoy versus hindcast Hs show a correlation coefficient of 0.98 and SI of 0.01. Estimated bias and RMSE are 0.01 and 0.01 respectively, both revealing a better agreement between the model and observations with PE of 9.0%. The MPI is also high enough (0.99) indicating that the model could simulate Hs very well at OB10 location. Samiksha et al. [38] have reported the results of WWIII validation using NIOT buoy data (DS5) for the period January to February 2006, which is located north of OB10. It indicates a satisfactory agreement between the model and buoy Hs with the R value of 0.92 using NCEP winds. In another validation exercise involving a long-term WWIII hindcast of 30 year period (1979-2009) using Climate Forecast System Reanalysis (CFSR) winds of NCEP has revealed that B, RMSE and SI varied from -0.97 to 0.90, 0.21 to 2.42 and 0.09 to 0.35 respectively between the model (Hs) and the NDBC buoy measurements in the Atlantic (Gulf of Mexico buoys) and Pacific (Hawaii buoys) Oceans [41].

In this case, Tc also showed reasonably a better correlation (R=0.89) between buoy measurements and WWIII hindcast. Here, the mean of observed Tc (buoy OB10) and WWIII hindcast deviate by 0.4 s for the observed/predicted range of 3.9 to 8.9 s. The SI of 0.11 for Tc indicates a good fit between the observed and hindcast Tc, using WWIII. The model hindcast and the observed Tc show a bias of -0.51, which is within a well acceptable range. The values of RMSE, PE and MPI are 0.53, 8.9% and 0.92 respectively. Therefore, all the above estimated statistics reveal a very good overall agreement between the model and buoy (OB10) observations excepting for few observations as seen from Figure 16.

Despite significant departures noted, the validation and performance evaluation of WWIII gave reliable results. From the validation with buoy measurements, it is demonstrated that the lower wave heights are not properly estimated in WWIII. The neglect of atmospheric stratification effects when converting wind speeds to the wind stress fields driving WWIIIcould be a possible reason for this. Another feature noted is that there exits larger deviation in Hs at locations DS1, SW1, SW4 and SW6. WWIII is a deep-water model,

6.1. Significant wave height (Hs in m)		
Sl. No.	**Statistical estimates**	**Bay of Bengal**
		OB10
1.	Mean (Buoy)	1.1
2.	Range (Buoy)	0.4 – 2.1
3.	Mean (WWIII)	1.2
4.	Range (WWIII)	0.5 – 1.9
5.	R	0.98
6.	SI	0.01
7.	B	0.01
8.	RMSE	0.01
9.	PE	9.0
10.	MPI	0.99
6.2. Mean wave period (Tc in s)		
1.	Mean (Buoy)	5.1
2.	Range (Buoy)	3.9 – 8.4
3.	Mean (WWIII)	5.6
4.	Range (WWIII)	4.4 – 9.0
5.	R	0.89
6.	SI	0.11
7.	B	-0.51
8.	RMSE	0.53
9.	PE	8.9
10.	MPI	0.92

***R:** Correlation Coefficient, **SI:** Scatter Index, **B:** Bias, **RMSE:** Root Mean Square Error, **PE:** Percentage Error &**MPI:** Model Performance Index.*

Table 6: Statistics of the comparison of WWIII model wave parameters with NIOT buoy measurements in the Bay of Bengal during January 2009 using QuikSCAT/ NCEP blended winds as shown in figure 16.

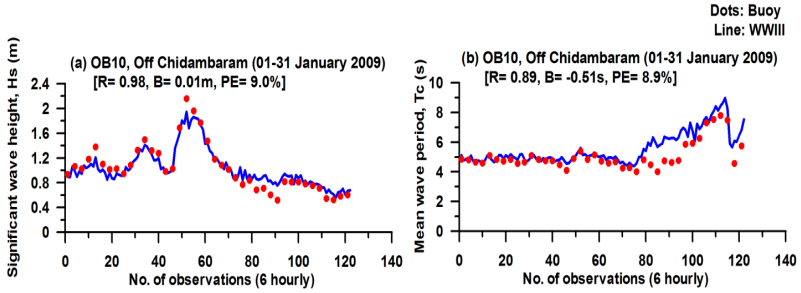

Figure 16: Comparison between the observed (NIOT buoy) and predicted wave parameters at 6 hourly intervals for the period January 2009 using QuikSCAT/ NCEP Blended winds

which can predict waves accurately up to 30 m water depth since they include crude shallow water equations, which does not satisfy near-shore wave transformations. However, the deep water hindcasts have been compared with the buoy observations at 16 to 24 m in the absence of measurements at preferable locations where water depth is more than 30 m. It was seen in most cases the PE values around 20% excepting in few cases where it was higher. Therefore, by considering the buoy data from such locations bordering 30 m of water depth were found to be useful to assess and evaluate the extent of agreement between the models (PE around 20%) and buoy at deeper than 15 m, which is the limiting depth for near-shore wave transformations.

Effect of Different Wind Fields Forcing on the Performance of Wave Model

The accuracy of the wave model outputs is highly dependent on the quality of wind inputs. Hence, the effect of different wind fields on the performance of the wave model has been evaluated. The two different winds products used are the ERA-40 and the QuikSCAT NCEP blended winds. The comparison of model outputs using buoy measurements (Figures 12-15) revealed notable deviations at many locations in the North Indian Ocean. The deviations in Hs and Tc using ERA-40 winds could be possibly due to the inaccuracy in the input wind fields. Hence, the blended wind field were considered in this study to force the wave model for selected buoys in the Arabian Sea and Bay of Bengal. The buoys considered in the validation of WWIII model outputs are DS1 (off Goa), and DS2 (off Lakshadweep) in the Arabian Sea and SW6 (off Chennai port) in the Bay of Bengal.

Figure 17 shows the comparison between the observed (buoys) and predicted wave parameters (Hs and Tc) at 6 hourly intervals for

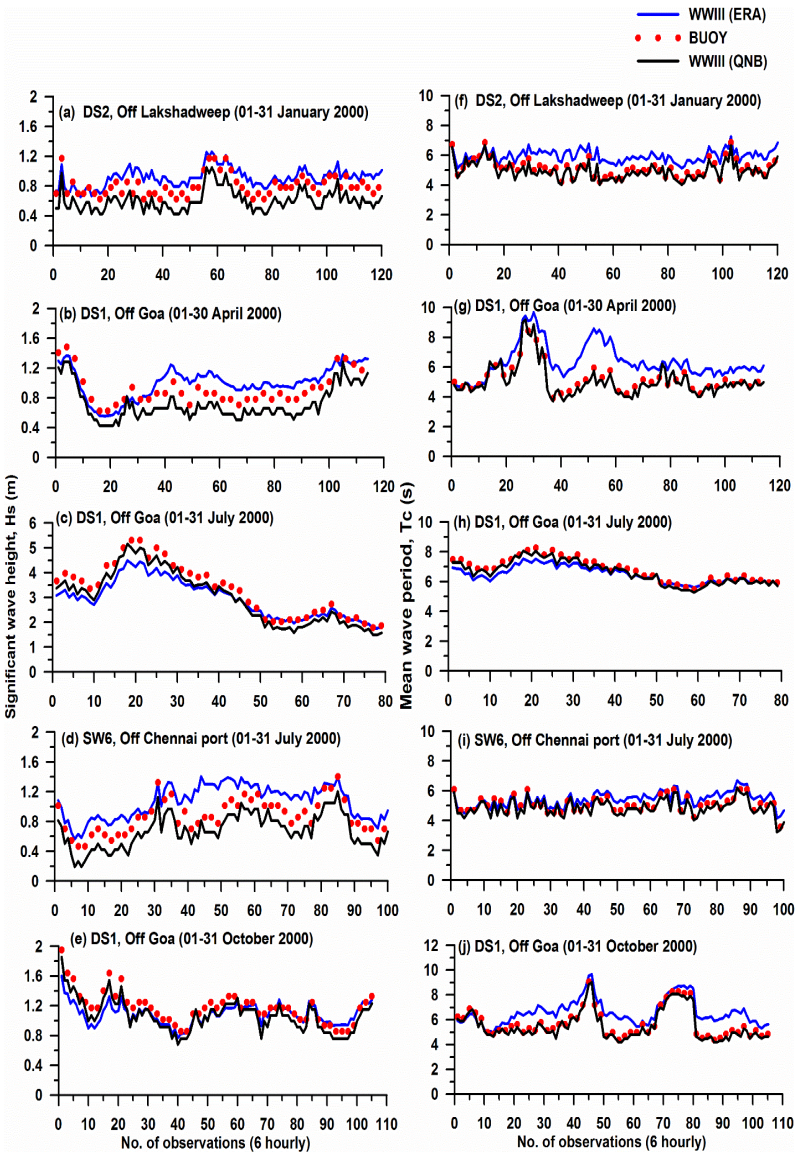

Figure 17: Comparison between the observed (NIOT buoys) and predicted wave parameters at 6 hourly intervals for selected buoys in the Indian Seas (January, April, July & October 2000) using two different wind forcing's (ERA-40 and QuikSCAT/NCEP Blended winds).

7.1. Significant wave height (Hs in m) WWIII (ERA) / WWIII (QNB)						
Sl. No.	**Statistical Estimates**	**January 2000**	**April 2000**	**July 2000**		**October 2000**
		DS2	**DS1**	**DS1**	**SW6**	**DS1**
1.	R	0.90/ 0.94	0.81/ 0.92	0.98/ 0.97	0.88/ 0.95	0.89/ 0.96
2.	B	-0.11/ 0.12	-0.08/ 0.16	0.36/ 0.14	-0.19/ 0.20	0.08/ 0.15
3.	PE	12.1/ 6.6	14.1/ 8.1	11.1/ 4.3	18.2/ 9.3	8.9/ 5.2
7.2. Mean wave period (Tc in s) WWIII (ERA) / WWIII (QNB)						
1.	R	0.80/ 0.96	0.71/ 0.98	0.98/ 0.99	0.89/ 0.98	0.85/ 0.99
2.	B	-0.80/ 0.09	-1.11/ 0.05	0.33/ 0.05	-0.35/ 0.06	-0.87/ 0.10
3.	PE	13.6/ 3.6	17.5/ 2.5	5.1/ 1.9	6.8/ 2.9	14.3/ 3.5
***R:** Correlation Coefficient, **B:** Bias and **PE:** Percentage Error*						

Table 7: Statistics of the comparison of WWIII model wave parameters with buoy measurements in the Arabian Sea and Bay of Bengal using different wind products as shown in figure 17.

selected buoys in the Indian Seas (January, April, July & October 2000) using two different wind fields (ERA-40 and QuikSCAT/NCEP Blended winds). In the Figure 17, WWIII (ERA) and WWIII (QNB) denotes the wave simulations using ERA-40 and QuikSCAT-NCEP blended winds respectively. The statistics of the comparison of the response of the model to two different wind fields is as shown in Table 7. The WWIII model comparisons using blended winds represented strong correlations (R>0.9); revealing that blended winds could simulate Hs and Tc at the buoy locations with higher accuracies when compared with the simulations results using ERA-40 winds. At the DS2 location, during January 2000, there is a significant decrease in the PE from 12.1 to 6.6% and 13.6 to 3.6 % for Hs and Tc respectively. During April 2000, in comparison to ERA 40 winds, the blended winds performed better with low PE (8.1%). At the SW6 location, the ERA-40 winds overestimated the Hs with a PE of 18.2%; while with the application of blended winds the comparison shows a good match with low bias and PE (9.3%). From the Figure 17, it is seen that the comparisons of Hs using ERA-40 winds are overestimated at the buoy locations considered (DS1, DS2 and SW6). It is to be noted that by using blended winds the WWIII model simulated Hs were in good match at the buoy locations with appreciable accuracy having lower bias and PE <10%. The over prediction of Tc using ERA-40 winds during January, April and October 2000 is notably reduced at thebuoy locations DS1 and DS2 with very low bias and PE <4%. The results of this study (Table 7) shows better statistical estimates, which indicate that agreement between simulated and observed wave parameters (Hs and Tc)is appreciably more accurate with the use of blended winds compared with ERA-40 winds. Hence, the model outputs obtained here are consistent with the measurements qualitatively.

Based on the performance evaluation and the statistical estimates it is inferred that the WWIII model performed well during all periods (January, April, July and October 2000) using blended winds. Despite being a shallow water location (SW6 buoy), the blended winds could reproduce Hs and Tc with much better accuracy as compared with ERA-40 winds. At the buoy locations, in this study the quality of blended winds played an important role in simulating the wave fields realistically, while the comparisons using ERA-40 winds showed moderate performances only. It is noted that during the fair-weather season, the study area would be dominated by long swells and the representation of swell propagation in model physics could be a possible reason for deviations at the buoy location. Apart from wind forcing, many other factors such as wave model physics, numeric and model grid resolution can affect the model performance. These studies indicate the impact and use of higher-frequency winds to force the wave model to yield realistic/accurate wave model outputs. The wave model results may suffer, without high quality wind forcing fields, even given the correct physics.

Conclusions

In the Indian Ocean from 50°E to 100°E and 0°N to 30°N; simulations using the state-of-the-art third generation model WAVEWATCH III have been demonstrated by utilizing the ERA-40 and QuikSCAT/NCEP Blended wind fields and the boundary conditions from the global run to predict uncertainty connecting the model performance. The significant wave height and mean wave period obtained from the WWIII simulations were validated against buoy measurements. The validation of WWIII with NIOT buoys gave satisfying results, irrespective of the input winds used. In the North Indian Ocean, the Model Performance Index varied from 0.86 to 0.99 and Percentage Error ranging from 3.1 to 18.8% considering most of the cases for January, June/July and October excepting April. Except the higher model estimates of significant wave height at few buoy locations in the Arabian Sea and Bay of Bengal, there is no significant difference in the comparison of the predicted and observed wave parameters. Generally, in the month of April, winds are generally found to be low and variable, which could not accurately reproduce the observed sea-state, as in the present study. This is the most likely reason for higher discrepancies between the wave model and the measurements in April, which is the pre-monsoon period. Apart from the quality of input winds, wave model physics, model grid resolution, numeric can contribute to the performance of the model at the study location. The impact of two different wind field products on the wave hindcast performance was also evaluated in this study. The numerical results revealed that the blended winds are more suitable in comparison with ERA-40 winds of modelling the waves in the Arabian Sea and Bay of Bengal. The results also show that wave model output is critically sensitive to the choice of the wind field product, such that the quality of the wind fields is reflected in the quality of the wave predictions. Hence, the present study suggests that, WWIIII model predictions are reliable with minimum uncertainty for the Indian Seas using the analysed wind fields such as ERA-40 and QuikSCAT/NCEP Blended wind fields. The study further aims to validate the model with available continuous measurements in the North Indian Ocean for longer periods, which will help in developing a hindcast database useful for user community dealing with various oceanographic and research applications.

Acknowledgements

The authors express their sincere thanks to Director, NPOL; Director, SAC and Group Head, Ocean Sciences for their encouragement and support provided to carry out this work. This is a part of the Ph.D. work of Umesh P. A., carried out at Naval Physical and Oceanographic Laboratory (NPOL), DRDO, Cochin under a collaborative project between NPOL and Space Applications Centre (SAC), Ahmedabad (Project: NPOL/SAC-II). They are extremely thankful to fellow scientists of Data Management Division, Ocean Science Group, NPOL for their timely support and encouragement. They are also grateful to Director, NIOT (National Institute of Ocean Technology, Chennai) as well as the Director, INCOIS (Indian National Centre for Ocean Information Services, Hyderabad) who have provided wave data for this study.

References

1. Richard AA, Kaihatu J, Hsu LY, Dykes JD (2002) The Integrated Ocean Prediction System (IOPS). Oceanography 15: 67-76.
2. Umesh PA, Swain J, Panigrahi JK (2007) Prediction of wind and wave induced ambient noise in the sea. J Acoust Soc India 34: 89-104.
3. Swain J, Umesh PA, Harikrishnan M (2010) Role of Oceanography in Naval Defence. Indian J Geo-Mar Sci 39: 631-645.
4. WAMDI Group (1988) The WAM model - A third generation ocean wave prediction model. J Phys Oceanogr 18: 1775-1810.
5. Komen GJ, Cavaleri L, Donelan M, Hasselmann K, Hasselmann S, et al. (1994) Dynamics and modelling of ocean waves. Cambridge University Press, UK, p: 554.
6. Tolman HL (1999) User manual and system documentation of WAVEWATCH III version 1.18. Tech. Note 166, NOAA/NWS/NCEP/OMB, 110.
7. Booij N, Holthuijsen LH, Ris RC (1999) A third-generation wave model for coastal regions. 1. Model description and validation. J Geophys Res 104: 7649-7666.
8. Rusu E (2011) Strategies in using Numerical Wave Models in Ocean/Coastal Applications. J Mar Sci Tech 19: 58-75.
9. Balakrishnan Nair TM, Sirisha P, Sandhya KG, Srinivas K, Sanil Kumar V, et al. (2013) Performance of the ocean state forecast system at Indian National Centre for Ocean Information Services. Curr Science 105: 175-181.
10. Balakrishnan Nair TM, Remya PG, Harikumar R, Sandhya KG, Sirisha P, et al. (2014) Wave forecasting and monitoring during very severe cyclone Phailin in the Bay of Bengal. Curr Sci 106: 1121-1125.
11. Sandhya KG, Balakrishnan Nair TM, Bhaskaran PK, Sabique L, Arun N, et al. (2014) Wave forecasting system for operational use and its validation at coastal Puducherry, east coast of India. Ocean Eng 80: 64-72.
12. Cavaleri L (2006) Wave modelling – where to go in the future. Bull American Meteor Soc 87: 207-214.
13. Cavaleri L (2009) Wave modeling-missing the peaks. J Phys Oceanogr 39: 2757-2778.
14. Janssen PAEM (2008) Progress in ocean wave forecasting. J Comput Phys 227: 3572-3594.
15. Tolman HL (2009) User Manual and System Documentation of WAVEWATCH III TM Version 3.14. Technical Note MMAB Contribution 276: 220.
16. Tolman HL, Chalikov DV (1996) Source terms in a third-generation wind-wave model. J Phys Oceanogr 26: 2497-2518.
17. Battjes JA (1994) Shallow water wave modeling. In: Proceedings of International Symposium: Waves – Physical and Numerical Modeling, Vancouver, M. Isaacsonand M. Quick (Edn), University of British Columbia, pp: 1-24.
18. Shemdin P, Hasselmann K, Hsiao SV, Herterich K (1978) Non-linear and linear bottom interaction effects in shallow water: In turbulent fluxes through the sea surface. Wave Dynamics and Prediction. NATO Conf. 1: 347-372.
19. Snyder RL, Dobson FW, Elliot JA, Long RB (1981) Array measurements of atmospheric pressure fluctuations above surface gravity waves. J Fluid Mech102: 1-59.
20. Hasselmann S, Hasselmann K, Allender JH, Barnett TP (1985) Computations and parameterizations of the nonlinear energy transfer in a gravity-wave spectrum - Part II: parameterizations of the nonlinear energy transfer for application in wave models. J Phys Oceanogr 15: 1378-1391.
21. Hasselmann K, Barnett TP, Bouws E, Carlson H, Cartwright DE, et al. (1973) Measurements of wind–wave growth and swell decay during the Joint North Sea Wave Project (JONSWAP). Deutsche Hydrographische Zeitschrift 8: 1-95.
22. Uppala SM, Kallberg PW, Simmons AJ, Andrae U, Da Costa Bechtold V, et al. (2005) The ERA-40 re-analysis. Q J Royal Meteor Soc 131: 2961-3012.
23. Chin TM, Milliff RM, Large WG (1998) Basin-scale, high-wave number sea surface wind fields from a multiresolution analysis of scatterometer data. J Atmos Oceanic Technol 15: 741-763.
24. Milliff RF, Large WG, Morzel J, Danabasoglu G, Chin TM (1999) Ocean general circulation model sensitivity to forcing from scatterometer winds. J Geophys Res 104: 11337-11358.
25. Kalnay E, Kanamitsu R, Kistler R, Collins W, Deaven D, et al. (1996) The NCEP/NCAR 40-year reanalysis project. Bull American Meteor Soc 77: 437-471.
26. Prem kumar K, Ravichandran M, Kalsi SR, Sengupta D, Gadgil S (2000) First results from a new observational system over the Indian Seas. Curr Sci 78: 323-330.
27. Jossia JK, Rajesh G, Latha G, Premkumar K (2010a) Ready Reckoner for wind and wave climate at selected locations in Indian Seas. Volume I: Arabian Sea. Published by National Institute of Ocean Technology (NIOT), Ministry of Earth Sciences, Chennai, p: 234.
28. Jossia JK, Rajesh G, Latha G, Premkumar K (2010b) Ready Reckoner for wind and wave climate at selected locations in Indian Seas. Volume II: Bay of Bengal. Published by National Institute of Ocean Technology (NIOT), Ministry of Earth Sciences, Chennai, p: 197.
29. Bonjean F, Lagerloef GSE (2002) Diagnostic model and analysis of the surface currents in the tropical Pacific Ocean. J Phys Oceanogr 32: 2938-2954.
30. Romeiser R (1993) Global Validation of the Wave Model WAM Over a One-Year Period Using Geosat Wave Height Data. J Geophys Res 98: 4713-4726.
31. Ris RC, Holthuijsen LH, Booij N (1999) A third-generation wave model for coastal regions: 2. Verification. J Geophy Res Oceans 104: 7667-7681.
32. Padilla-Hernandez R, Perrie W, Toulany B, Smith PC (2007) Modeling of two Northwest Atlantic storms with third-generation wave models. Wea Forecasting 22: 1229-1242.
33. Korres G, Papadopoulos A, Katsafados P, Ballas D, Perivoliotis L, et al. (2011) A 2-year intercomparison of the WAM-Cycle4 and the WAVEWATCH-III wave models implemented within the Mediterranean Sea. Mediterr Mar Sci 12: 29-152.
34. Remya PG, Kumar R, Basu S, Sarkar A (2012) Wave hindcast experiments in the Indian Ocean using MIKE 21 SW model. J Earth Syst Sci 121: 385-392.
35. Hastenrath S, Lamb PJ (1979) Climatic atlas of the Indian Ocean, Part-I: Surface climate and atmospheric circulation. Madison: The University of Wisconsin Press, USA, p: 117.
36. Young IR, Holland GJ (1996) Atlas of the oceans: Wind and wave climate. Pergamon, Elsevier Science Ltd, New York, USA, 241.
37. MontoyaRD, Arias AO, Royero JCO, Ocampo-Torres FJ (2013) A wave parameters and directional spectrum analysis for extreme winds. Ocean Eng 67: 100-118.
38. Samiksha SV, Vethamony P, Aboobacker VM, Rashmi R (2012) Propagation of Atlantic Ocean swells in the north Indian Ocean: a case study. Nat Hazards Earth Syst Sci 12: 3605-3615.
39. Sabique L, Annapurnaiah K, Balakrishnan Nair TM, Srinivas K (2012) Contribution of Southern Indian Ocean swells on the wave heights in the Northern Indian Ocean - A modeling study. Ocean Eng 43: 113–120.
40. DHI (2009) MIKE 21 wave modelling user guide. Danish Hydraulic Institute (DHI) Water and Environment, Denmark, p: 14.
41. Chawla A, Spindler DM, Tolman HL (2013) Validation of a thirty year wave hindcast using the Climate Forecast System Reanalysis winds. Ocean Model 70: 189-206.